REPORT DOCUMENTATION PAGE

AFRL-SR-BL-TR-00-

0301

reviewing
information

1. AGENCY USE ONLY *(Leave blank)*	2. REPORT DATE	3. REPORT TYPE AND DATES COVERED
	February 2000	FINAL TECHNICAL REPORT 1 Mar 98 - 30 Nov 99

4. TITLE AND SUBTITLE
INSTRUMENTATION FROM STUDIES OF FUNDAMENTAL ISSUES IN MICROWAVE PROCESSING OF NANOGRAINED CERAMICS

5. FUNDING NUMBERS
F49620-98-1-0340

61103D
3484/US

6. AUTHOR(S)
YUVAL CARMEL

7. PERFORMING ORGANIZATION NAME(S) AND ADDRESS(ES)
UNIVERSITY OF MARYLAND
INSTITUTE OF PLASMA RESEARCH
DEPT OF MATERIALS AND NUCLEAR ENGINEERING
COLLEGE PARK, MD 20742

8. PERFORMING ORGANIZATION REPORT NUMBER

9. SPONSORING/MONITORING AGENCY NAME(S) AND ADDRESS(ES)
AIR FORCE OFFICE OF SCIENTIFIC RESEARCH
801 N. RANDOLPH STREET, ROOM 732
ARLINGTON, VA 22203-1977

10. SPONSORING/MONITORING AGENCY REPORT NUMBER

11. SUPPLEMENTARY NOTES

12a. DISTRIBUTION AVAILABILITY STATEMENT
APPROVED FOR PUBLIC RELEASE, DISTRIBUTION IS UNLIMITED

12b. DISTRIBUTION CODE

13. ABSTRACT *(Maximum 200 words)*

The equipment purchased is intended to greatly enhance the diagnostics capabilities, and will be used to investigate several fundamental issues related to the effects of microwaves on diffusion, grain growth, and energy deposition within porous polycrystalline and single-crystal ceramic materials, including nanograin ceramics. The following items were acquired, delivered, installed and are in use in our laboratories: 1) Thermal conductivity system; 2) Vector network analyzer; 3) Microhardness tester; 4) Stereo microscope.

20000712 010

14. SUBJECT TERMS	15. NUMBER OF PAGES
	29
	16. PRICE CODE

17. SECURITY CLASSIFICATION OF REPORT	18. SECURITY CLASSIFICATION OF THIS PAGE	19. SECURITY CLASSIFICATION OF ABSTRACT	20. LIMITATION OF ABSTRACT
U	U	U	

UNIVERSITY OF
MARYLAND
INSTITUTE FOR PLASMA RESEARCH

Energy Research Building #223
Paint Branch Drive
College Park, Maryland 20742-3511
301.405.4951 TEL 301.314.9437 FAX

~~March 1, 2000~~

June 14, 2000

Ms. Wendy Veon
~~Dr. Alexander Pechenik~~
Air Force Office of Scientific Research/NA
801 N. Randolph Street, Room 732
Arlington, VA 22203-1977

RE: AFOSR Grant No. F49620981034O

Ms. Veon
Dear ~~Dr. Pechenik:~~

a copy
Enclosed please find ~~the original and two copies~~ of the Final Technical Report on the abovenamed DURIP project, "Instrumentation for Studies of Fundamental Issues in Microwave Processing of Nanograin Cermics."

We thank you for your support of this research effort.

Sincerely,

Carol A Bellamy

Carol Bellamy
Editorial Assistant

cc: M. Hess, IPR
Y. Carmel (PI), IPR
P. Hagen, ORAA

INSTRUMENTATION FOR STUDIES OF FUNDAMENTAL ISSUES IN MICROWAVE PROCESSING OF NANOGRAIN CERAMICS

Final report

AFOSR DURIP Grant Number F496209610456

Incorrect Grant # Resubmitted w/ correct # 6/15/00 cb

Submitted to

Air Force Office of Scientific Research

Submitted by

Institute for Plasma Research

and

Dept. of Materials and Nuclear Engineering

University of Maryland

College Park, MD 20742

February 2000

INSTRUMENTATION FOR STUDIES OF FUNDAMENTAL ISSUES IN MICROWAVE PROCESSING OF NANOGRAIN CERAMICS

Final report

AFOSR DURIP Grant Number F49620-98-10340

Submitted to

Air Force Office of Scientific Research

Submitted by

Institute for Plasma Research

and

Dept. of Materials and Nuclear Engineering

University of Maryland

College Park, MD 20742

February 2000

INSTRUMENTATION FOR STUDIES OF FUNDAMENTAL ISSUES IN MICROWAVE PROCESSING OF NANOGRAIN CERAMICS

EXECUTIVE SUMMARY

This is a final report for AFOSR instrumentation Grant (DURIP) number F49620-98-10340 The program is entitled "Instrumentation for Studies of Fundamental Issues in Microwave Processing of nanograin Ceramics".

The equipment purchased is intended to greatly enhance the diagnostics capabilities, and will be used to investigate several fundamental issues related to the effects of microwaves on diffusion, grain growth, and energy deposition within porous polycrystalline and single-crystal ceramic materials, including nanograin ceramics.

The following items were acquired, delivered, installed and are in use in our laboratories:

1) Thermal conductivity system

2) Vector network analyzer

3) Microhardness tester

4) Stereo microscope

As an example, we enclose a preprint of a very recent manuscript describing the use of the thermal conductivity system purchased during this grant to characterize the thermal conductivity of various ceramic powders, including nano powders, during processing *(Thermal Conductivity of ZnO: From Green to Sintered State, by T. Olorunyolemi, A. Birnboim, Y. Carmel, O. Wilson, Jr., I. Lloyd, University of Maryland, College Park, MD and S. Smith and R. Campbell Holometrix, Bedford, MA).*

As a second example, we enclose a preprint of a manuscript dealing with the densification characteristics of nanopowders *(Measurement o Densification of Zinc Oxide Compacts Using an Optical, Noncontact, Noninvasive Extensometer, by T. Olorunyolemi, R. Tolbert, O. Wilson, Y. Carmel, I. Lloyd, G. Xu and A. Jaworsky, Univ. of MD, College Park).*

Journal

J. Am. Ceram. Soc., 83 (4) 000–000 (2000)

Measurement of Densification of Zinc Oxide Compacts Using an Optical, Noncontact, Noninvasive Extensometer

Tayo Olorunyolemi,* Renee Tolbert, Otto Wilson Jr.,* Yuval Carmel,* Isabel Lloyd,* Gengfu Xu, and Allen Jaworski

Institute for Plasma Research, University of Maryland, College Park, Maryland 20742

An optical noninvasive, noncontact extensometer was used to measure the shrinkage of zinc oxide powder compacts during sintering. Powder compacts were uniaxially and isostatically pressed from micrometer, submicrometer, and nano powders and sintered in a thermal oven at temperatures up to 1100°C. The nanometer-size sample started to densify at ~400°C, about 200°C below the densification threshold of the micrometer-size sample. The results are in good agreement with those obtained using a contact dilatometer.

I. Introduction

The search for ceramic materials with improved properties has led to the development of novel processing methods. One of the active areas of research in ceramic processing is the use of microwave energy to densify ceramics.[1–4] While a number of reports have shown that microwave processing of ceramics can be used to achieve better microstructural control and enhanced properties, the mechanism behind these results is still unclear. One unique way to better understand microwave processing of ceramics is to monitor their densification in a microwave furnace *in situ*.

Densification experiments are most commonly carried out using conventional dilatometers,[5,6] which use a pushrod system to maintain contact with the sample. The expansion or shrinkage of the sample is then measured as a function of temperature or time at a known heating or cooling rate. However, it is undesirable to use a traditional dilatometer in a microwave furnace for three reasons. First, it is difficult to accommodate a pushrod type of apparatus within a microwave furnace since it requires parts and shields that accommodate moving parts. Second, the dilatometer components may interact with the microwaves and thus affect the microwave field and temperature distribution within the oven and the sample being processed. Third, the mechanical stresses associated with contact dilatometry could affect the otherwise pressureless process. The use of a noncontact, noninvasive system avoids the potential problems mentioned above. This paper describes the use of an optical extensometer to remotely measure the shrinkage of powder compacts. The results compare favorably with those obtained using a conventional (contact) pushrod dilatometer.

II. Experimental Procedure

The extensometer is an optical system.[7] It consists of a light source and a detector. The detector consists of the lens, the gauge length adapter, and the measuring head. The lens on the instrument is designed for samples that are 75 mm in length. A gauge length adapter allows samples from 5 to 30 mm to be measured. A schematic diagram of the setup for the instrument, showing the different components, is depicted in Fig. 1.

To measure shrinkage, the detector uses the contrast between the edges of the sample and the environment. Therefore, the sample must be colored or color modified before shrinkage can be measured. Usually, the two edges of the sample are painted or they may have flags attached to them. At high temperature, none of these methods can be used. However, we found that the shrinkage of our samples could be measured without marking the edges. The contrast provided by the color of our samples (off-white) was enough to allow the image to be formed on the detector.

The distance between the sample and the detector is known as the working distance. The working distance is dependent on the nominal length of the sample, l_0, the lens, and the gauge length adapter. Before the start of the experiment, the working distance must be determined and adjusted in order to obtain a clear and well-focused image on the detector. However, the sample remains "in focus" during the entire sintering process, even while undergoing densification. The working distance for our particular equipment is shown in Table I for different sample sizes.

For a typical experiment, the extensometer is positioned on one side of a tube furnace and the light source is positioned opposite the extensometer. The sample is placed on top of a porous alumina holder which is designed as a semicylinder so that it can be moved in and out of the furnace. The sample is positioned inside the

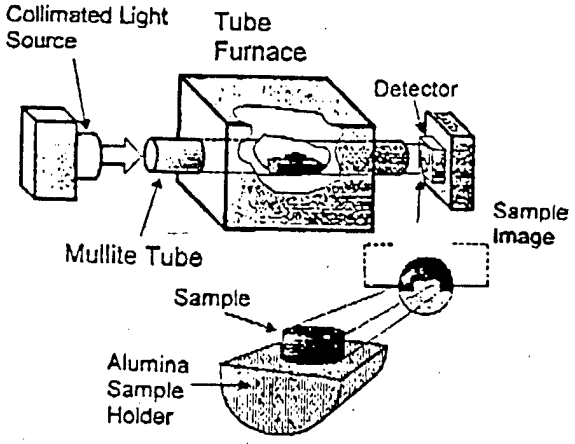

Fig. 1. Schematic diagram of the optical extensometer for measuring densification. The extensometer measures shrinkage by optically identifying the edges of the sample.

D. R. Clarke—contributing editor

Manuscript No. 189288. Received June 16, 1999; approved September 22, 1999. Presented at the 101st Annual Meeting of the American Ceramic Society, Indianapolis, IN, April 27, 1999 (Dielectric Materials and Devices, Paper No. S-E-054-99).

Supported by the Air Force Office of Scientific Research (AFOSR), Structural Ceramics Division, under Grant No. F49620-97-10270 and partially supported by the Naval Research Laboratory.

*Member, American Ceramic Society.

Table I. Working Distance for a Sample with Nominal Length (l_o) between 5 and 30 mm

l_o (mm)	Working distance (mm)
5	357.5
10	360
15	362.5
20	365
25	367.5
30	370

furnace so that the distance between the sample and the extensometer is the previously determined working distance. The light source is turned on, and the extensometer is adjusted until the image of the sample is centered on the viewfinders.

Commercial powders of different particle size ZnO—nano (NanoTek, 20 nm), submicrometer (Zinc Corporation of America, 0.17–0.24 μm), and micrometer (Cerac, Inc., 1 μm)—were used for the experiments. The sample disks were pressed uniaxially in a die at 30 MPa and then pressed isostatically at 300 MPa. Sample disks were dried in an oven at 120°C for 1 h to remove physisorbed water before the densification experiments. The sintering experiments in the standard pushrod dilatometer (Orton, Cincinnati, OH) were carried out under identical conditions.

III. Results and Discussion

Results obtained for sintering experiments carried out at a heating rate of 3°C/min are shown in Fig. 2. Experiments carried out under the same conditions in a pushrod dilatometer are shown in Fig. 3. Experiments were carried out at other heating rates (see Table II), and results similar to those carried out at 3°C/min (shape and magnitude) were obtained. It should be noted that similar curves were obtained in the experiments carried out using the extensometer and the pushrod dilatometer. Results of the experiments on nano-size samples using the dilatometer and the extensometer are compared in Fig. 4. The overlaid plots show excellent agreement between the values obtained using the two systems. The difference in the measured percentage shrinkage was less than 3% (±3%) of the standard dilatometer value at all temperatures. These results show that the extensometer can be used to monitor the densification of ceramics *in situ*.

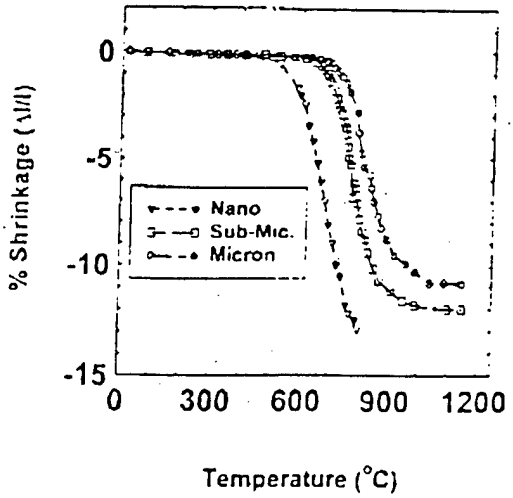

Fig. 2. Shrinkage versus temperature curves for ZnO compacts (three different particle sizes) obtained using the optical extensometer. Heating rate = 3°C/min.

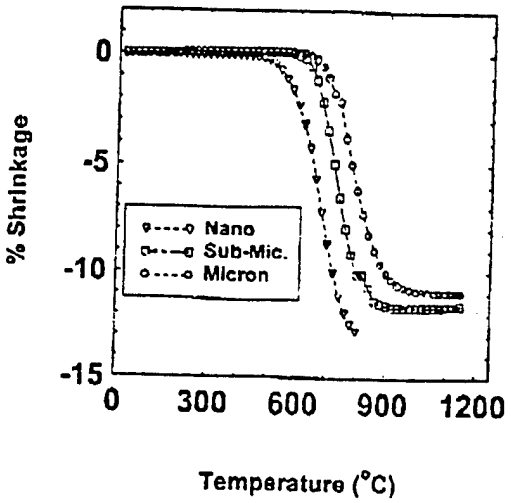

Fig. 3. Shrinkage versus temperature curves for ZnO compacts (three different particle sizes) obtained using a dilatometer. Heating rate = 3°C/min.

Table II. Sintering Experiments[†] Carried Out in This Study

Heating rate (°C/min)	Nano	Submicrometer	Micrometer
3	□	□	□
10	X	X	X
20	X	X	X

[†]Using conventional and optical dilatometry. The results for experiments with □ sign are presented.

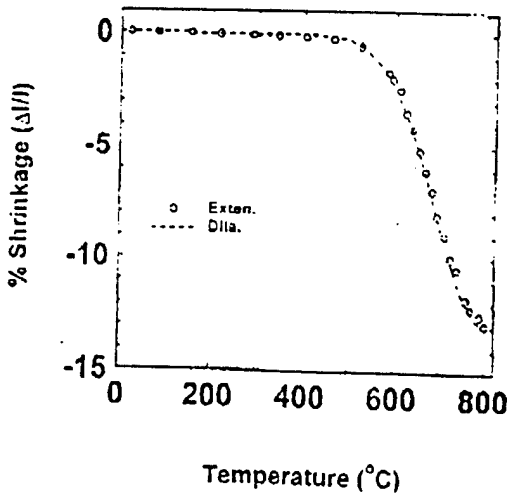

Fig. 4. Comparison between shrinkage of nano-sized ZnO carried out in a pushrod dilatometer and optical extensometer. The agreement between the two systems is better than ±3% shrinkage over the entire temperature range.

Note the differences in the sintering behavior of the samples of different particle sizes in both Figs. 2 and 3. The nano-size sample starts to densify at about 200°C before the micrometer-size sample. Recent work revealed that the thermal conductivity of ZnO is dependent on the particle size of the sample, with smaller grain samples having higher thermal conductivities.[4] Simulations of the thermal conductivity below the sintering threshold indicate that the interparticle necks in smaller particle size samples grow faster than in the larger particle size samples. The faster rate of neck growth in the smaller size samples will lead to earlier densification as observed in the present experiment. It is well known that heating

ceramics at high temperature for extended periods leads to excessive grain growth. Therefore, the use shrinkage controlled sintering cycles could lead to the manufacture of novel materials for applications where small grain sizes are desired.

Our research group is currently working on integrating the extensometer into our microwave furnace. We have a software, developed in-house, that is being used to control our microwave furnace. A section is included in the software that will use the shrinkage of ceramics as a feedback loop system to control the sintering process. Therefore, we will be able to do rate-controlled, as well as temperature-controlled, sintering. Rate-controlled sintering experiments,[9,10] in which materials are sintered at a constant optimum shrinkage rate, have been shown to lead to improved material properties. However, it has not been possible to do this in a microwave environment because of the problems enumerated earlier. The optical extensometer provides a novel method to introduce rate-controlled sintering into microwave systems. The combination of the densification experiments (rate- and temperature-controlled) and the characterization of the microstructure during different experimental conditions will help in developing novel materials and in explaining some of the "microwave effects" in ceramics.

IV. Summary

It is very difficult to use a standard pushrod dilatometer in a multimode microwave cavity. The good agreement between shrinkage rates observed using an optical extensometer and a standard dilatometer indicate that the optical extensometer can be used as a dilatometer in a microwave environment. With appropriate feedback loops, such a system can be used for intelligent control during microwave processing. In addition, experiments using both systems showed that ZnO nanopowder started to densify about 200°C below those of more conventional powders. This was not unexpected because of the difference in particle size. It confirmed earlier work measuring thermal conductivity of particle compacts during heating.[8]

Acknowledgments:

We want to thank Evan Pert and David Gershon for useful discussions.

References

[1]W. H. Sutton, "Microwave Processing of Ceramic Materials," *Am. Ceram. Soc. Bull.*, 68, 376 (1989).

[2]D. E. Clark, D. C. Folz, R. L. Schulz, Z. Fathi, and A. D. Cozzi, "Recent Developments in the Microwave Processing of Ceramics," *MRS Bull.*, 18 (11) 41 (1993).

[3]M. Willert-Porada, "The Origin of 'Microwave Effects' in Microwave Sintering of Ceramics and Composites"; p. 44 in *First World Congress on Microwave Processing, Abstract Book* (January 5–9, 1997, Lake Buena Vista, FL).

[4]W. B. Snyder Jr., W. H. Sutton, M. F. Iskander, and D. L. Johnson (Eds.), Materials Research Society Symposium Proceedings, Vol. 189, *Microwave Processing of Materials*, Materials Research Society, Pittsburgh, PA, 1991.

[5]G. Agarval and R. F. Speyer, "Effect of Rate Controlled Sintering on Microstructure and Electrical Properties of ZnO Doped with Bismuth and Antimony Oxides," *J. Mater. Res.*, 12, 2447 (1997).

[6]F. J. T. Lin and L. C. De Jonghe, "Microstructure Refinement of Sintered Alumina by a Two-Step Sintering Technique," *J. Am. Ceram. Soc.*, 80, 2269 (1997).

[7]The Cooke Corporation, Optical Direct Extensometer, Internal Publication, 1995.

[8]A. Birnboim, T. Olorunyolemi, and Y. Carmel, "Calculating the Thermal Conductivity of Heated Compacted Ceramic Powders," unpublished work.

[9]H. Palmour III, M. L. Huckabee, and T. M. Hare; pp. 205–15 in *Sintering—New Developments*. Edited by M. M. Ristic, Plenum Press, New York, 1978.

[10]G. Agarval, R. F. Speyer, and W. S. Hackenberger, "Microstructural Development of ZnO Using a Rate-Controlled Sintering Dilatometer," *J. Mater. Res.*, 11, 671 (1996)

Keywords: densification; zinc oxide

ADVANCE COPY J. Am Cer. Soc. as a communication. June 99

Thermal Conductivity of ZnO: From Green to Sintered State

T. Olorunyolemi, A. Birnboim, Y. Carmel, O. Wilson, Jr., I. Lloyd
University of Maryland, College Park, MD 20742

S. Smith and R. Campbell
Holometrix, 25 Wiggins Avenue, Bedford, MA 01730

ABSTRACT

The thermal conductivity of ZnO with different particle sizes (micron, submicron and nano) was measured using the laser flash technique. As the "green" samples were heated from room temperature to 600 °C (and 1000 °C) and then cooled down to room temperature, the thermal conductivity was measured in situ. A model for inter-particle neck growth was developed based on mass transfer to the neck region of a powder as a result of known temperature gradient. By combining this model with a three-dimensional numerical code, the thermal conductivity of ZnO was calculated. Excellent agreement between the theoretical calculation and experimental data was found.

"Presented at the 101st Annual Meeting of the American Ceramic Society, Indianapolis, IN, April 28, 1999 (Computation, Simulation and Modeling, Paper No. S-B-051-99)
"Supported by Air Force Office of Scientific Research Grant No. F496209710270."

I. INTRODUCTION

The search for materials with improved thermal, electrical and mechanical properties has led to increased interest in ceramics, which can be prepared with different properties. Knowledge of thermal conductivity is essential in applications involving heat generation or high temperatures. For example, thermal conductivity determines the reliability of devices where heat dissipation and thermal shock resistance are major considerations[1,2]. In the processing of ceramics, thermal conductivity is important in designing novel sintering techniques, like microwave processing, where high heating rates, $\leq$ 1000 °C/min, may be attained[3,4]. Large temperature gradients in these materials can cause density gradients, leading to non-uniformity in grain size distribution and properties, as well as quality degradation and cracking.

Because of its importance in the design and manufacture of a wide range of ceramic engineering materials, extensive theoretical and experimental studies have been carried out on the thermal conductivity of ceramics. However, there is limited number of studies in the literature that attempt to study the relationship between the thermal conductivity and the microstructure of materials starting from the "green" state. The dearth of data can be attributed to the difficulty in measuring thermal conductivity for a shrinking sample.

On a macroscopic scale, the presence of pores and other defects in the ceramic body leads to a reduction in thermal conductivity. A small degree of porosity will strongly influence the phonon mean free path and severely limit the thermal conduction. Apart from pores, the thermal conductivity of ceramic materials is affected by other macroscopic effects, like microcracking, anisotropy and the presence of moisture.

This paper examines the microstructure-thermal conductivity relationship in ceramic materials, starting with the earliest stages of sintering before densification is measurable. In this study, two sets of experiments were done using ZnO samples. In the first set, "green" samples were heated to 600 °C (below the densification threshold for micron and submicron particles). In the second set, nano size green ZnO samples were heated to 1000 °C (well above the sintering threshold). In situ measurements of the thermal conductivity were performed for all systems during a cycle of heating and cooling.

The goal of this work is to compare the experimentally observed thermal conductivity to a theoretical model to develop an understanding of the microstructure-thermal conductivity relationship. Section II contains a brief description of the experimental setup for in-situ measurement of the thermal conductivity, as well as sample preparation techniques. The results of the measurements and a comparison between the experimental results and thermal conductivity calculations based on neck growth are presented in section III. Conclusions are presented in section IV.

II. EXPERIMENTAL

Thermal diffusivity and specific heat measurements were carried out using a Thermaflash 2200 laser flash instrument[5]. Primary components in the measurement section of the apparatus include a pulsed Nd:glass laser, a tantalum furnace for sample temperature control, and an infrared (IR) detector. When the temperature of the small, disk-shaped sample has stabilized inside the furnace, the laser is fired, depositing a small pulse of energy on the front surface of the sample. As heat diffuses to the back surface,

the time-temperature response of this back surface is monitored by the IR detector, and recorded digitally by the data acquisition system. Using literature-based routines[6–9], the automation software analyzes rear-face temperature data, making corrections for heat loss or pulse width effects, if any, to compute the sample's thermal diffusivity.

For the specific heat measurement, a reference sample (Pyroceram 9606) of known specific heat was measured under the same conditions and at the same temperature as the test sample. By comparing the relative thermal response for reference and test samples, specific heat of the ZnO is calculated.

Thermal conductivity is then determined from the measured thermal diffusivity, specific heat and bulk density of the sample using the equation

$$K = \alpha \rho c_p \qquad (1)$$

where α is thermal diffusivity, K is thermal conductivity, c_p is specific heat and ρ is bulk density.

Commercial ZnO powders, herein referred to as "nano" (NanoTek, ~20nm), "submicron" (Zinc Corporation of America, 0.17 - 0.24μm), and "micron" (Cerac, Inc., ~1μm) powders to indicate predominant particle size, were uniaxially pressed at room temperature to 37 MPa. Sample disks approximately 12 mm in diameter and 2 mm thick, were used for thermal diffusivity and specific heat measurements. Before the measurements, both test and reference samples were coated on both surfaces with graphite in order to produce equivalent optical properties—a critically important requirement for accurate specific heat determination. The use of graphite also enhances the signal to noise ratio in diffusivity measurements.

Measurements were carried out on the first set of samples at room temperature. The temperature was then ramped at 3 °C /min to 200 °C and another measurement was then taken. Measurements were also taken at 400 and 600 °C. As the samples were cooled to room temperature, measurements were made successively at 500, 400, 200 and 25 °C.

For the second set of experiments, a nanometer particle size sample was heated from room temperature to 1000 °C at 4°C /min. Thermal diffusivity and specific heat measurements were carried out at regular intervals during heat-up and cool-down.

III. RESULTS AND DISCUSSION

A. Samples Heated to 600 °C

Curves of thermal conductivity vs. temperature for the three sets of ZnO samples (micron, sub-micron and nano), measured as they were heated to 600 °C and cooled back to 25 °C, are shown in Figure 1. Note that above 400 °C the thermal conductivity of the nano particle size increases faster with increasing temperature than that of the sub-micron and the micron particle size samples. This difference is a result of the lower sintering temperature of nano size ZnO.

Figure 2 shows the thermal conductivity of the micron size ZnO plotted as a function of time, along with its thermal history. The nano and sub-micron size samples have the same general features as the micron size sample shown in Figure 2. The measured thermal conductivity exhibits complex behavior. It decreases slightly as temperature is increased to ~ 200 °C, but beyond this point the trend reverses, and thermal conductivity is seen to increase with further increases in temperature. On cool down, the thermal

conductivity exhibits a strong hysteresis, and thermal conductivity continues to increase, even as temperature is reduced. As explained below, this radical change in temperature dependence suggests a transition from a thermal conductivity characteristic of powders to one that is increasingly dominated by solid conduction in the continuous phase of the consolidating ceramic.

i. Thermal conductivity

For ceramic powders, the earliest stage of sintering is characterized by smoothing of particle surfaces, rounding of interconnected pores, and inter-particle bonding. All these effects are known to result in little or no change of density or volume. Certain properties of ZnO powders, however, like surface area and sound velocity, are observed to change at temperatures well below the sintering threshold, sometimes as low as 200 °C[10-14]. Figure 2 shows that the thermal conductivity also changes well below the sintering threshold; the measured values are not constant, but increase with increasing temperature and time.

We believe that the increase in thermal conductivity observed at temperatures well below the sintering threshold is driven most strongly by growth of the neck region surrounding the inter-particle contact points. To test this hypothesis, we used a model describing the growth of inter-particle necks. The results of the neck growth model, applied to the case of spherical particles, were combined with a three-dimensional code to simulate processes affecting the apparent thermal conductivity of a porous ceramic. Details of the model simulation and calculations have been reported elsewhere [15], but a brief review is given below.

The two-sphere model was used to model the growth of inter-particle necks. This is a popular model, and it has been used extensively to model the sintering behavior of ceramics.[16,17] It includes different diffusion mechanisms and paths for the processes taking place within and between the spheres. The model uses the particle radius, the neck radius, and the radius of curvature of the neck to develop a relationship for the neck growth at a given temperature. Incorporating the diffusion mechanism for the initial stage of heating, the following equation for the neck growth was developed:

$$\int X^6 dX = B \int \exp \frac{\Gamma}{T(t)} \left[-\frac{Q}{K_B T(t)} \right] \tag{2}$$

where X is the neck radius, Q is the activation energy for neck growth, K_B is Boltzmann's constant, and T(t) is the temperature at time t. B is defined as

$$B = 16 D_0 w \gamma \delta^3 R^3 / (\pi K_B) \tag{3}$$

where γ is surface energy, w is the width of diffusion region, δ^3 is the vacancy volume, R is the particle radius, and D_0 is the vacancy diffusion coefficient prefactor.

The above equation can be solved numerically for any temperature history using estimates and literature values for the parameters in the equation. The values used for these parameters, and their literature sources, are given in Table 1.

The simulation code calculates an effective heat flux produced by a particular temperature gradient imposed on the particles. For the general case of heat flow in a solid, Fourier's Law gives

$$q = - k \nabla T \qquad (4)$$

where k, the thermal conductivity, is the ratio of heat flux, q (W/m^2-K) to the temperature gradient, ∇T (K/m). Heat transport in porous materials can, in general, be a complex process involving several modes of heat transfer, including conduction through the solid phase, conduction through the interstitial gas, and radiative exchange between (or through) particles. For ZnO powders in the neck growth regime, calculations showed that conduction in the solid is by far the dominant mechanism, and the negligible contribution of other modes was not considered.

In the pre-sintering regime, two competing mechanisms influence the temperature dependence characteristic of the sample's thermal conductivity: conduction within the particles decreases with increasing temperature, as the rate of resistive phonon-phonon interactions increases; and conduction between particles increases as neck growth reduces contact thermal resistance. The relative strength of these two effects determines the character of the conductivity/temperature curve.

For the temperature regime modeled in the present work, the predominant effect on thermal conductivity is produced by the neck growth mechanism, which, in its early stage, leads to significantly enhanced inter-particle heat conduction. During this stage, in which no densification takes place, ($X/R << 1$), the model predicts that the increase in effective thermal conductivity is directly proportional to neck growth.

By combining the two-sphere model of inter-particle neck formation, the simulation, and the intrinsic thermal conductivity of dense ZnO as a function of temperature, one obtains the temperature dependence of the thermal conductivity. This

dependency is given in equation 5. Using this equation, the thermal conductivity of

$$K = 376.\frac{(14.2\,X/R + 0.154)}{T} \qquad (5)$$

micron size ZnO was calculated for temperatures below the sintering threshold. The simulated thermal conductivity as well as the experimental results are shown in Figure 3.

For the early stage of heating, before significant neck growth occurs, the simulation shows that the dominant influence on measured thermal conductivity of the pressed ZnO pellets is the intrinsic thermal conductivity of the ZnO particles. This explains the initial decrease in the measured thermal conductivity, since thermal conductivity of fully dense ZnO decreases with increasing temperature. As the temperature is increased above 350 °C, the simulation predicts a rapid growth of inter-particle necks and an associated increase in thermal conductivity, which was indeed observed. In addition, the model predicts that neck growth continues even after the temperature ramp is stopped at 600 °C, and continues to grow as the temperature is decreased to ~500 °C. As temperature is further reduced below 500 °C, the neck radius remains essentially constant, and the dominant factor affecting thermal conductivity is the strongly temperature-dependent conductivity of dense ZnO.

Our experimental results and model predictions are in agreement with the work of Whittemore and Varela[10], who showed that no shrinkage of ZnO (micron size) occurs below 600 °C, but also that the surface area of the sample decreased upon heating through this temperature range (below sintering). They attributed the decrease in surface area to neck formation.

ii. Particle size effects

The particle size of the starting material is important in determining the features of the final product. Our simulation shows the influence of the particle size on the growth rate of the neck and the thermal conductivity. The influence of the particle size on the grain growth is implicitly contained in equation 2, in which the constant B is proportional to R^3. Solving equation 2 for X/R shows that it is directly proportional to $R^{-4.7}$. This dependence predicts a faster growth in thermal conductivity for smaller particles. This model also corroborates our experimental results. As seen in Figure 1, the slope (derivative) of the thermal conductivity vs. temperature curve for the nano-sized sample is greater than those of the micron and the sub-micron size sample. Because of the faster neck growth of smaller size particles, the nano size sample is expected to start densifying at lower temperature. This is observed in densification experiments carried out on ZnO of different particle sizes, where the nano size sample starts to densify at ~ 400 °C, about 200 °C below the sintering (densification) threshold of the micron size sample. The densification experiments were carried out using an Orton 1600 dilatometer, and the results are presented in Figure 4.

Note that the thermal conductivity of the nano size sample (~ 9 W/mK) is much larger than that of the micron and submicron size samples (~ 3W/mK) heated to 600 °C and cooled back to room temperature. As discussed above and seen in Figure 4, the nano size sample starts to densify at ~400 °C. The measured thermal conductivity is therefore not in the region where there is only neck formation but where there is also some densification. Since our model was originally developed for the initial stage of sintering

where no densification takes place, it was not able to explain the effect of particle size on the thermal conductivity of samples when there is densification. Therefore, we modified the code developed for samples heated below sintering and used it to simulate the thermal conductivity of the nano-size sample. The modified code took account of the densification taking place between ~400 and 600 °C. The experimental data and the simulated results are plotted in Figure 5. The modified simulation correctly predicts the character of the thermal conductivity curve before and during the initial stages of densification.

B. Nano Samples Heated to Full Density

With the laser flash method, we were able to measure the thermal conductivity of ZnO from the "green" sample to the fully sintered material. This work is one of the few to measure thermal conductivity from the "green" to the fully dense state. The lack of literature data is due to the difficulty of measuring the thermal conductivity as the sample is shrinking. The sample holder used in this study was modified to maintain sample position relative to the measurement axis during shrinkage, and changes in sample dimensions and density were accounted for when calculating thermal diffusivity. The correction for dimensional changes was obtained from the dilatometry experiments presented in Figure 4.

The measured thermal conductivity for the green nano sample heated from room temperature to 1000 °C (full densification) is shown in Figure 6. Here again, for reasons discussed above, the thermal conductivity of the porous samples decreases slightly in the early stage of heating, before significant neck growth has occurred, due to the inverse

temperature dependence of the ZnO thermal conductivity. Neck growth results in increasing conductivity in the next stage, until the inverse temperature dependence once again comes to dominate above 800 °C, due to the elimination of pores during densification (which also eliminates radiative heat transfer).

Figure 7 shows thermal conductivity measurements for a fully sintered sample heated from room temperature to 1000 °C. Note the decrease in the thermal conductivity from 37 to 4 W/mK as the temperature is increased from room temperature 1000 °C. This is the thermal conductivity curve for fully dense ZnO previously referred to, which is similar in character to many ceramics in the temperature range over which resistive phonon-phonon interactions (umklapp processes) are the dominant scattering mechanism; the high end of the previous plot exhibits the same characteristic temperature dependence, indicative of the fully sintered state.

Conclusions

In this work, we have shown that thermal conductivity can be modeled and measured from the green state to the fully sintered state. This has potential applications in process control and the development of porous materials with tailored thermal conductivities. We have also shown that neck growth occurs at much lower temperatures than would be expected based on "traditional" sintering studies. This has implications with respect to thermal treatment of powders. In addition, we have shown that thermal conductivity measurements can serve as a sensitive probe of microstructure in ceramics, especially during the earliest stages of sintering where steady-state methods cannot be applied. Finally, we have shown that particle size effects on thermal

conductivity can be accurately simulated allowing prediction of densification behavior in new materials such as nanopowders.

Acknowledgment

The authors are grateful to Allen Jaworski for sample preparation and to David Gershon and Evan Pert for helpful discussions.

REFERENCES

[1]. A.H. Guenther and J.K. Mciver, "The Role of Thermal Conductivity in the Pulsed Laser Damage Sensitivity of Optical Thin Films," Thin Solid Films, **163**, 203 (1988)

[2]. K. Kokini and Y.R. Takeuchi, "Transient Thermal Fracture of an Interface Crack in the Presence of a Surface Crack ," J. Therm. Stresses, **17**, 63 (1994)

[3]. W. Sutton, "Microwave Processing of Ceramic Materials," Ceram. Bull. **68**, 376 (1989)

[4]. A. Birnboim and Y. Carmel, "Microwave Sintering of Complex Bodies," in press, J. Am. Ceram. Soc.

[5]. Thermal conductivity measurements were carried out in the laboratory of Holometrix (a division of Metrisa, Inc.) by R. Campbell and S. Smith.

[6]. W.J. Parker, R.J. Jenkins, C.P. Butler, and G.L. Abbott, "A Flash Method of Determining Thermal Diffusivity, Heat Capacity and Thermal Conductivity," J. Appl. Phys. **32**, 1679 (1961)

[7]. R.D. Cowan, "Pulse Method for Measuring Thermal Diffusivity at High Temperature," J. Appl. Phys. **34**, 926 (1963)

[8]. L.M. Clark III and R.E. Taylor, "Radiation Loss in the Flash Method for Thermal Diffusivity" J. Appl. Phys. **46**, 714 (1975)

[9]. J.A. Koski, "Improved Data Reduction Methods for Laser Pulse Diffusivity Determination with the Use of Minicomputers", in Proc. Eight Symp. On Thermophysical Properties, Vol. II, p.94 J.V. Sengers, Ed, Am. Soc. Mech. Eng., New York (1981)

[10]. O.J. Whittemore and J.A. Varela, "Initial Sintering of ZnO", Comm. Am. Ceram. Soc. C-154 (1981)

[11]. R.M. German and Z.A. Munir, "Surface Area Reduction During Isothermal Sintering," J. Am. Ceram. Soc. **59**, 379 (1976)

[12]. L. P. Martin, D. Dadon, M. Rosen, D. Gershon, K. I. Rybakov, A. Birman, J.P. Calame, B. Levush, Y. Carmel and R. Hutcheon, "Effects of Anomalous Permittivity on the Microwave Heating of Zinc Oxide," J Appl. Phys. **83**, 432 (1998).

[13]. L.P. Martin, D. Dadon, M. Rosen, D. Gershon, A. Birman, J.P. Calame, B. Levush, and Y. Carmel, "A Dielectric Mixing Law for Porous Ceramics Based on Fractal Boundaries", J. Appl. Phys. **80**, 3992 (1996)

[14]. L.P. Martin, D. Dadon, M. Rosen, D. Gershon, A. Birman, B. Levush, and Y. Carmel, "Ultrasonic and Dielectric Characterization of Microwave and Conventionally Sintered ZnO", J. Am. Ceram. Soc. **79**, 2652 (1996)

[15]. A. Birnboim, T. Olorunyolemi, and Y. Carmel, "Calculating the Thermal Conductivity of Heated Compacted Ceramic Powders," submitted to J. Am. Ceram. Soc.

[16]. M.N. Rahaman, "Ceramic Processing and Sintering," Marcel Dekker Inc. 1995

[17]. R. L Coble, "Initial Sintering of Alumina and Hematite," J. Am. Ceram. Soc. **41**, 55 (1958)

[18]. Y.S. Touloukian, R.W. Powell, C.Y. Ho, P.G. Klemens, "Theory of Thermal Conductivity of Nonmetallic Solids," Thermophysical Properties of Matter, The TPRC Data Series, Plenum, New York (1970)

[19] J.E. Parrott and A.D. Stuckes, "Thermal Conductivity of Solids," Applied Physics Series, J.W. Arrowsmith Ltd. 1975.

Figure captions

Figure 1: Thermal conductivity of "green" nano, submicron and micron particle size ZnO heated from room temperature to 600 °C at 3 °C/min.

Figure 2: Thermal conductivity of micron size ZnO plotted as a function of time. The temperature profile is also shown on the graph.

Figure 3: Measured and calculated thermal conductivity for the "green" micron size ZnO heated to 600 °C and then cooled to room temperature.

Figure 4: The densification curves for nano, submicron and micron ZnO. The densification experiments were carried out using an Orton 1600 dilatometer.

Figure 5: Measured and calculated thermal conductivity of "green" nano size ZnO heated to 600 °C and then cooled down to room temperature.

Figure 6: Thermal conductivity of "green" nano particle size ZnO heated from room temperature to 1000 °C.

Figure 7: Thermal conductivity of fully sintered ZnO (sample from Figure 3, cooled down to room temperature) heated from room temperature to 1000 °C.

Table caption

Table 1: Values of physical parameters used in the calculation of the thermal conductivity of micron size (conventional) ZnO.

Table 1; Values of physical parameters used in the calculation of the thermal conductivity of micron size (conventional) ZnO.

Parameter	Value	Notes
Grain Size, R	0.65 μm	Average particle radius
Width of diffusion region, w	0.4 nm	Reference 16 page 345
Surface energy, γ	0.1 J/m^2	Reference 16, page 448
Oxygen vacancy volume,δ^3	9.6×10^{-24}	Using 1.32 A as the radius of oxygen in ZnO molecule
Diffusion coefficient pre factor, D_o	0.01 m^2/sec	
Activation energy, Q/K_B	19000 K	Equivalent to 158 KJ/mole

Figure 1: Thermal conductivity of "green" nano, submicron and micron particle size ZnO heated from room temperature to 600 °C at 3 °C/min.

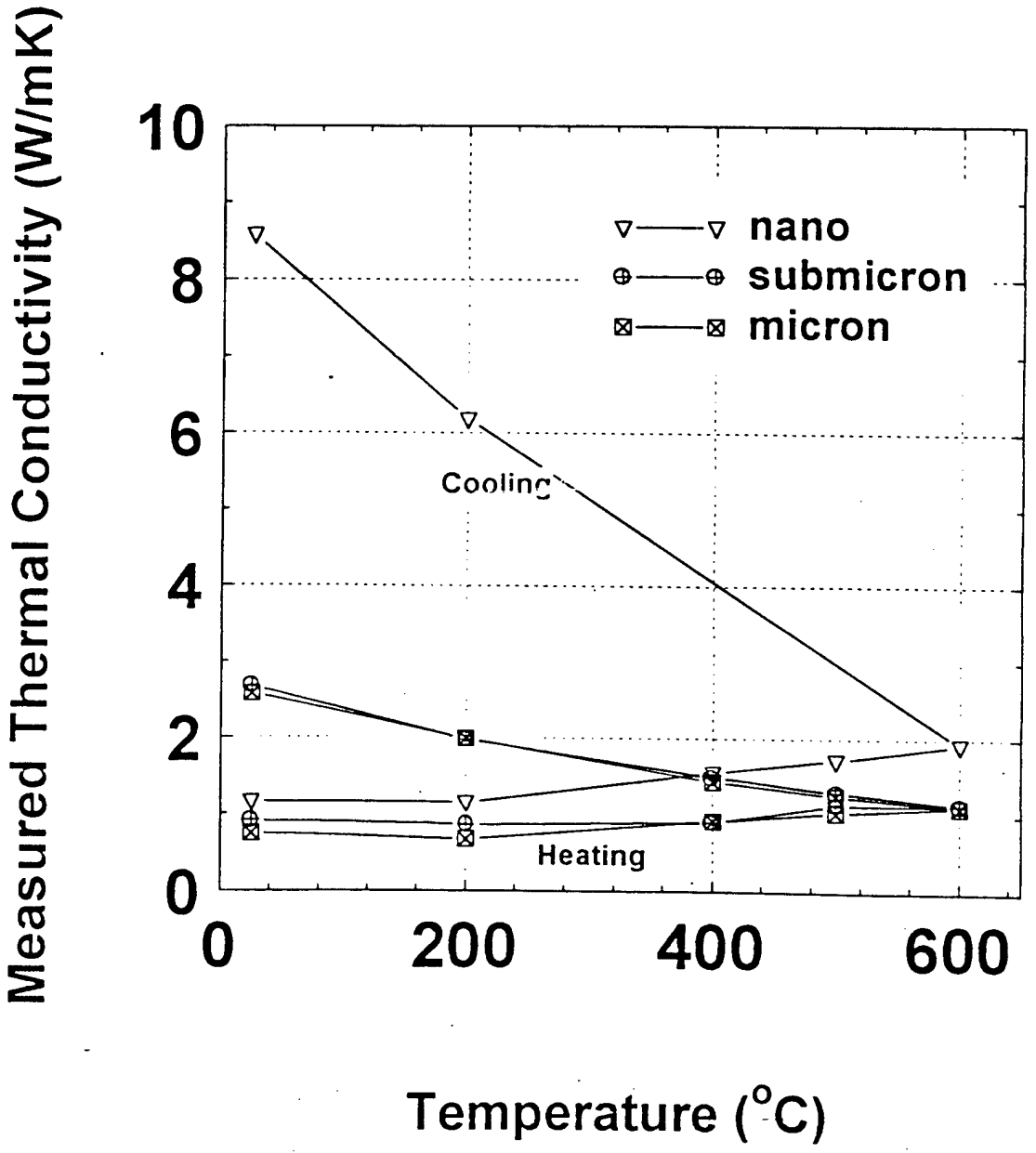

Figure 2: Thermal conductivity of micron size ZnO plotted as a function of time. The temperature profile is also shown on the graph.

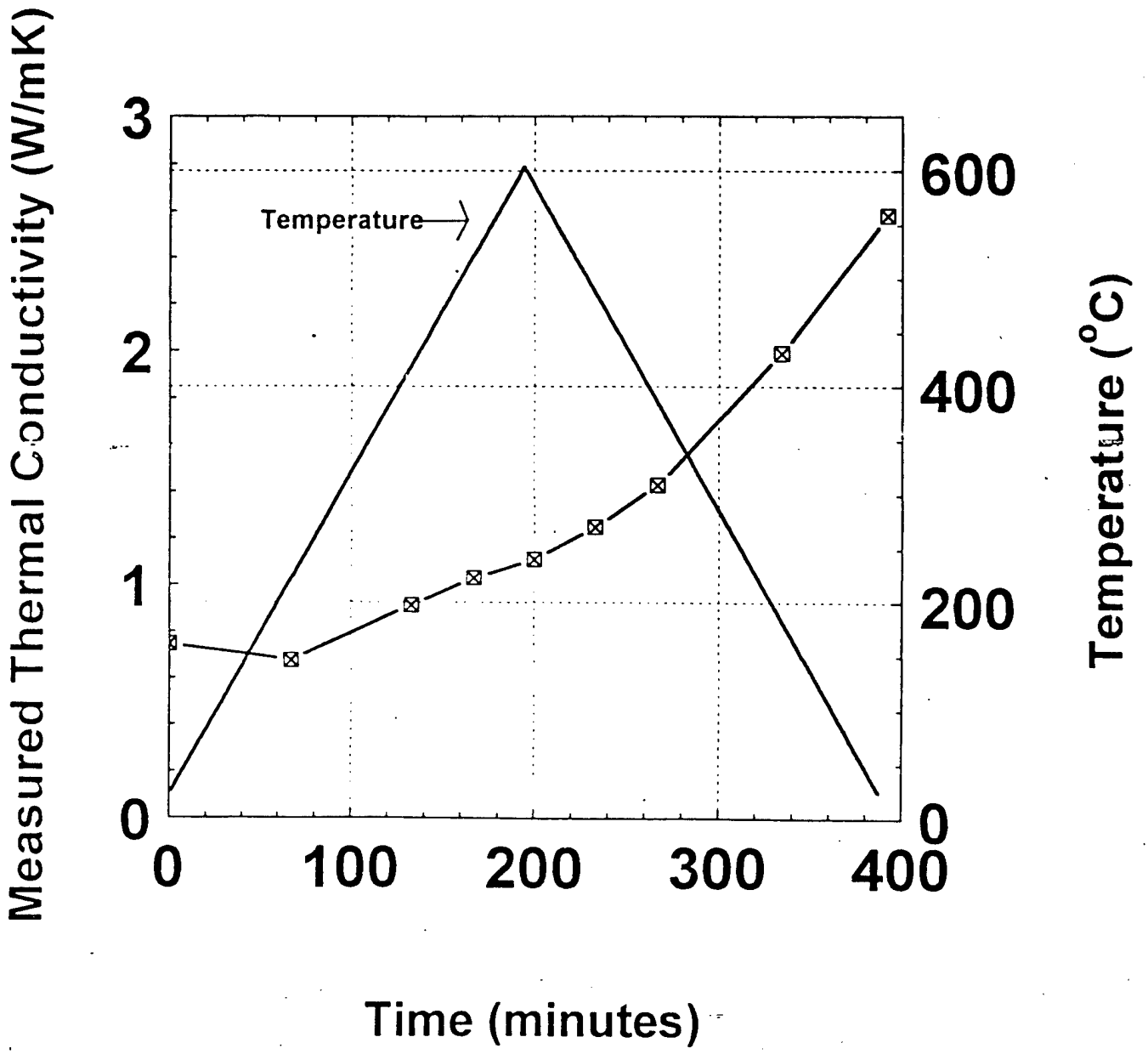

Figure 3: Measured and calculated thermal conductivity for the "green" micron size ZnO heated to 600 °C and then cooled to room temperature.

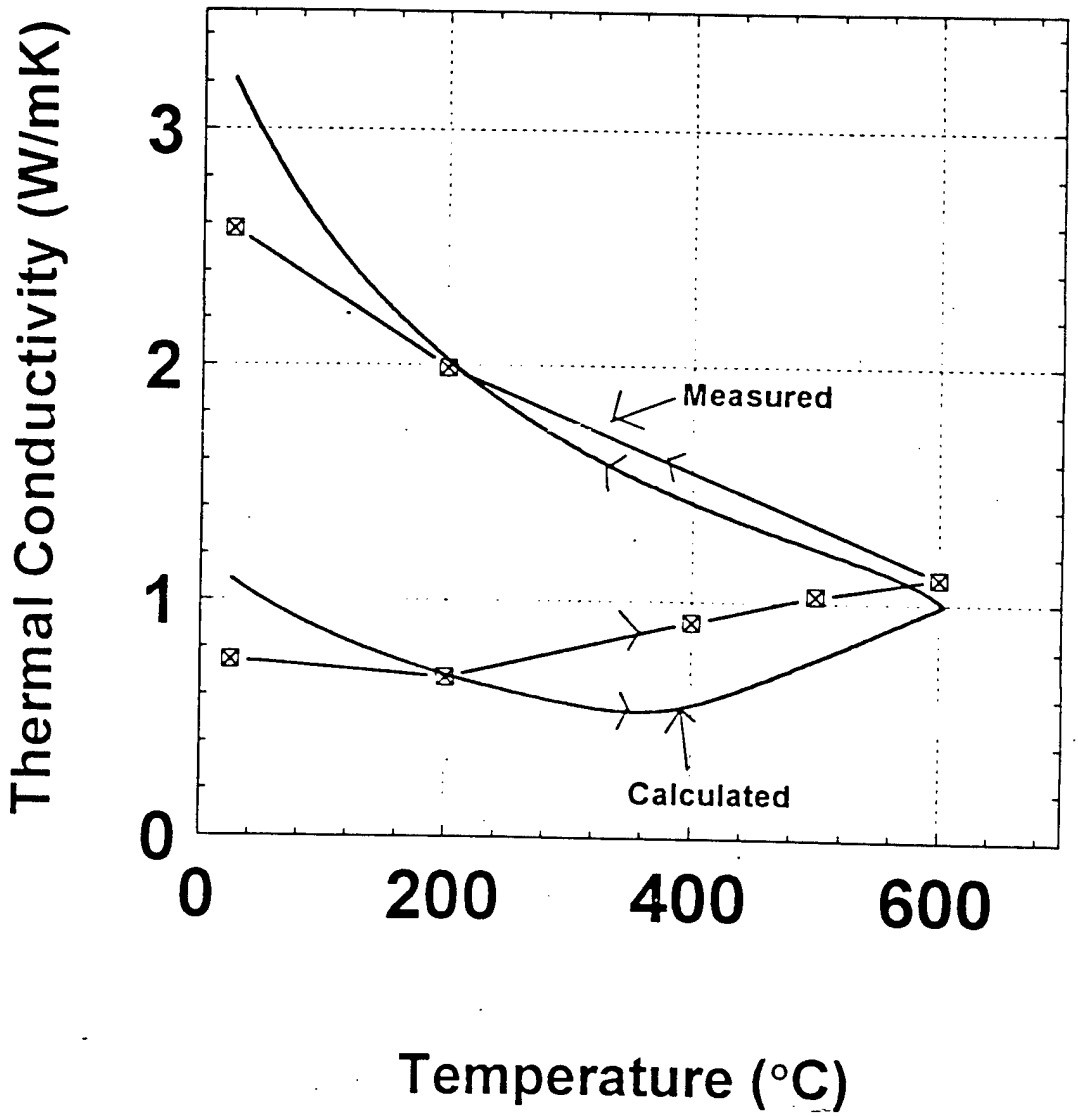

Figure 4: The densification curves for nano, submicron and micron ZnO. . The densification experiments were carried out using an Orton 1600 dilatometer.

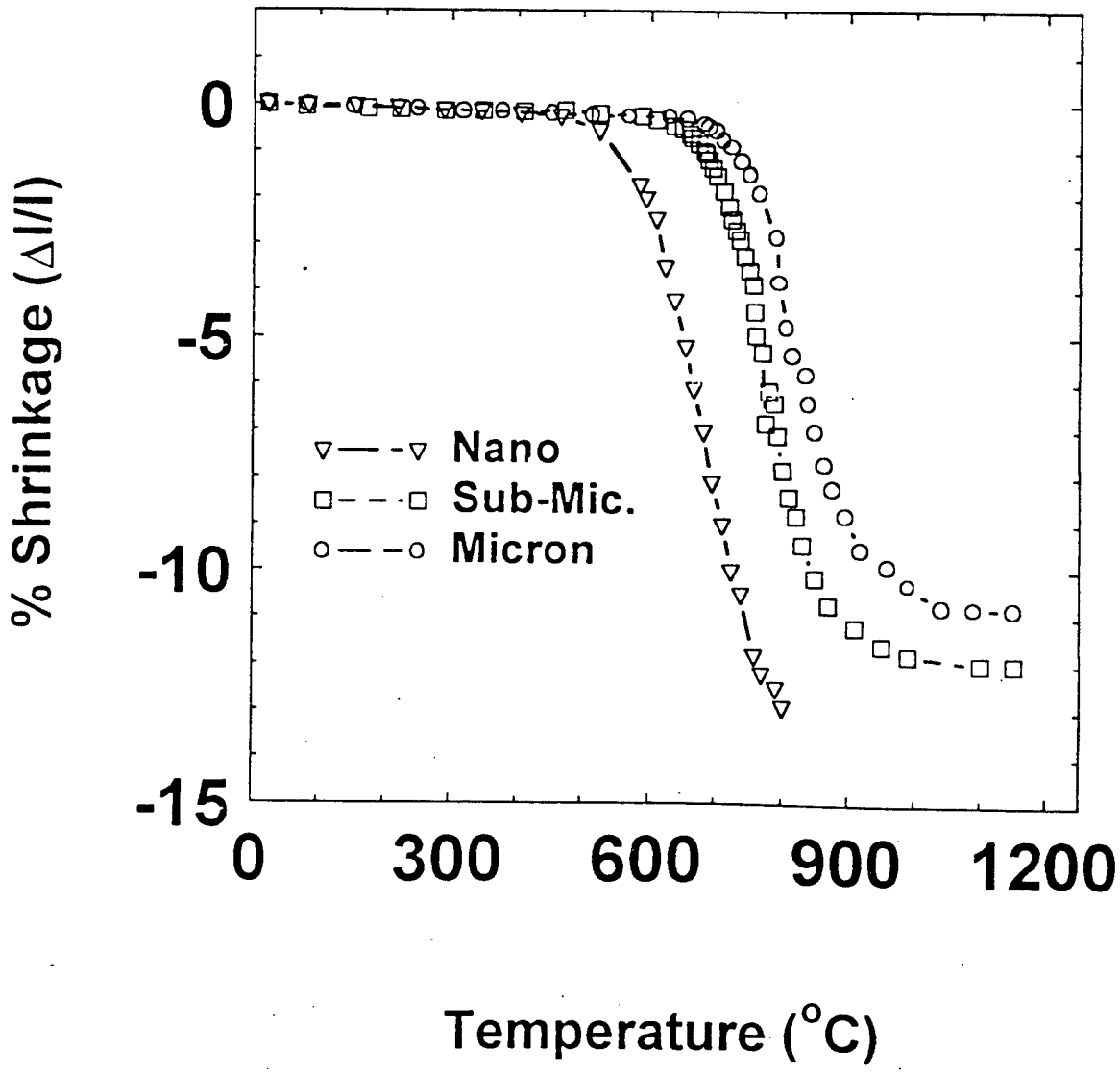

Figure 5: Measured and calculated thermal conductivity of "green" nano size ZnO heated to 600 °C and then cooled down to room temperature.

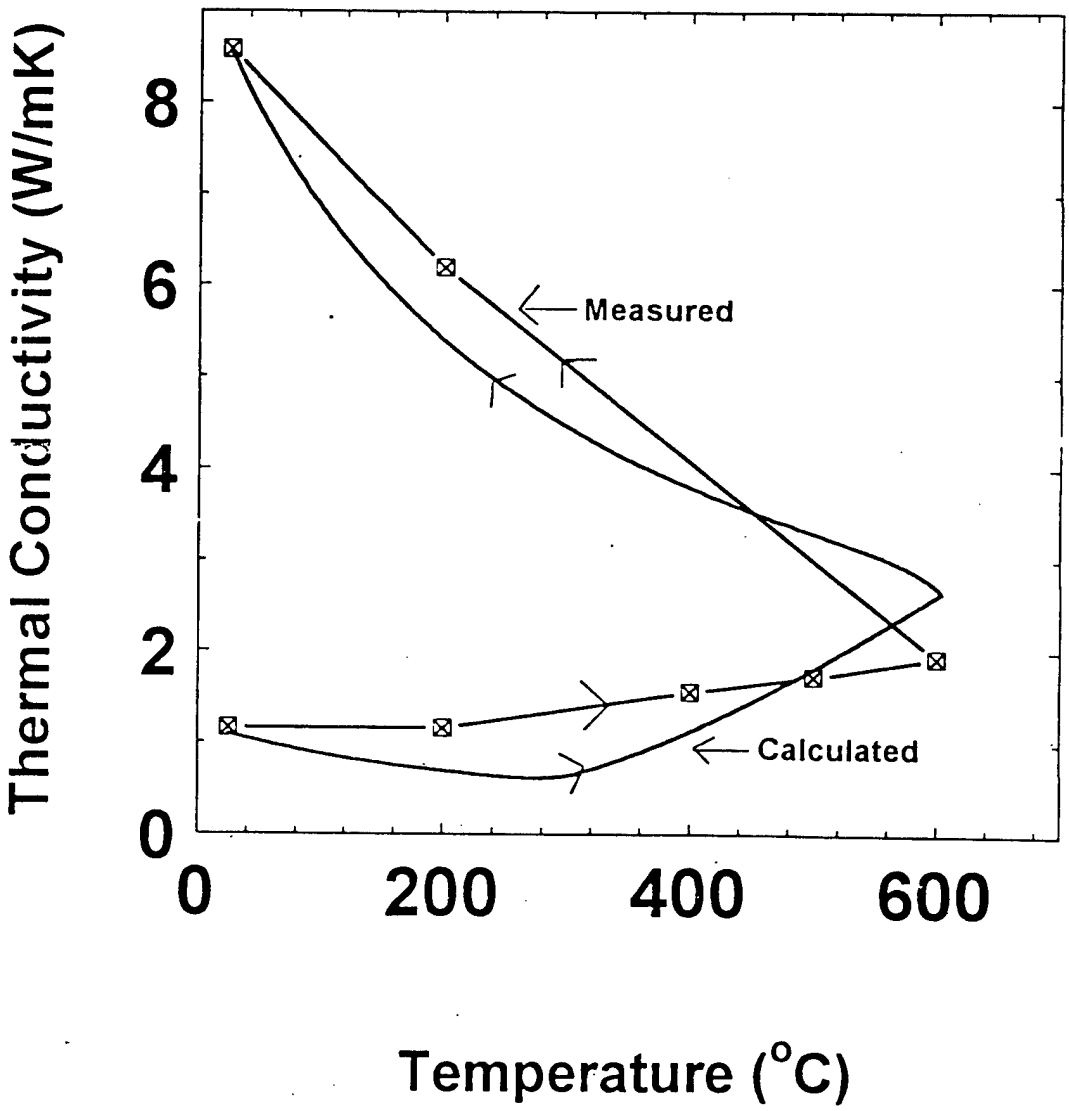

Figure 6: Thermal conductivity of "green" nano particle size ZnO heated from room temperature to 1000 °C.

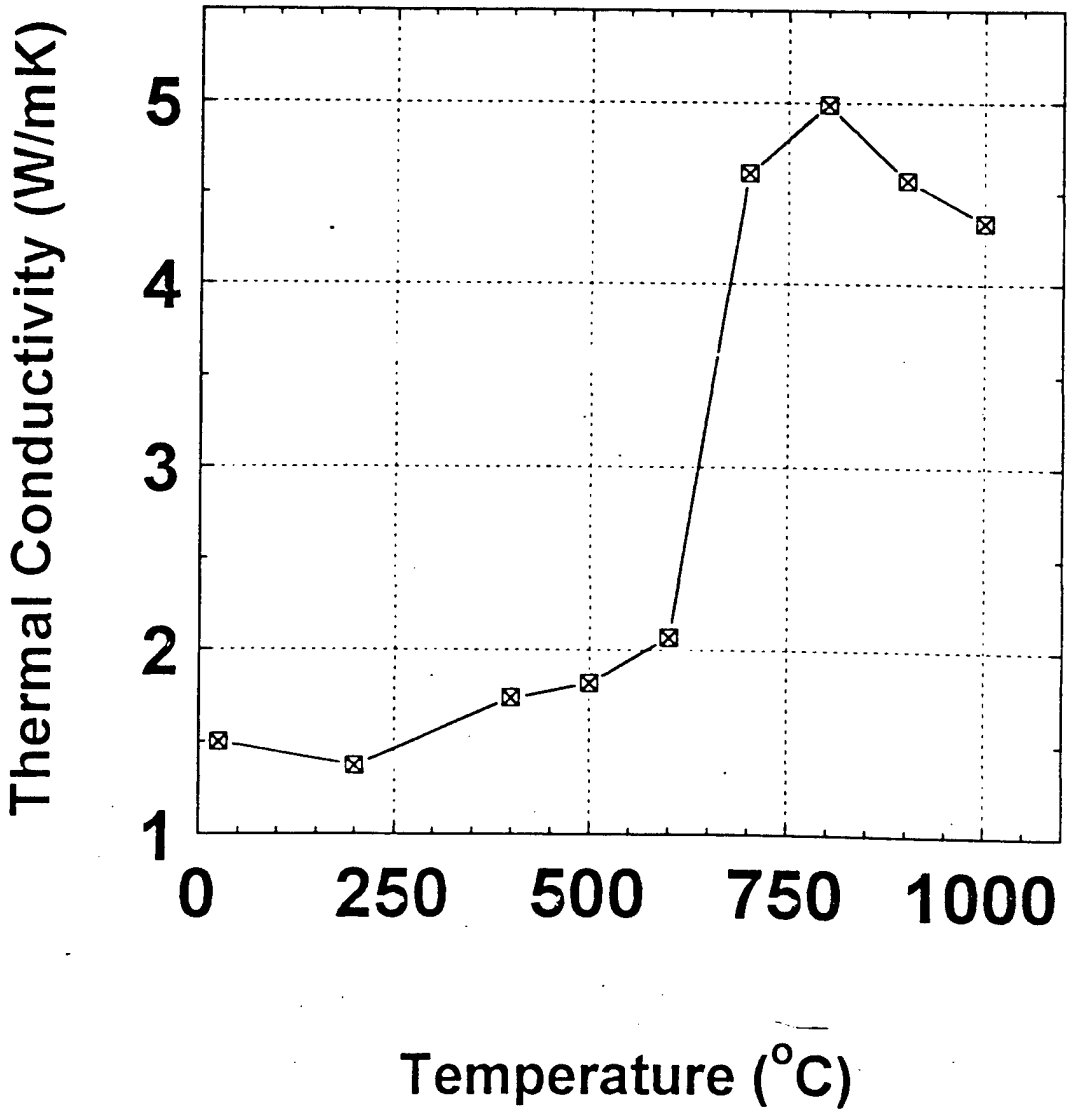

Figure 7: Thermal conductivity of fully sintered ZnO (sample from Figure 3, cooled down to room temperature) heated from room temperature to 1000 °C.